Physica B 459 (2015) 116–121

Contents lists available at ScienceDirect

Physica B

journal homepage: www.elsevier.com/locate/physb

Thermally-induced electronic relaxation in structurally-modified $Cu_{0.1}Ni_{0.8}Co_{0.2}Mn_{1.9}O_4$ spinel ceramics

O. Shpotyuk [a,b,*], V. Balitska [a,c], M. Brunner [d], I. Hadzaman [a,e], H. Klym [a,f]

[a] Institute of Materials, Scientific Research Company "Carat", 202, Stryjska Street, Lviv 79031, Ukraine
[b] Institute of Physics, Jan Dlugosz University, 13/15, al. Armii Krajowej, Czestochowa 42200 Poland
[c] Lviv State University of Vital Activity Safety, 35, Kleparivska Street, Lviv 79007, Ukraine
[d] Fachhochschule Köln/University of Applied Sciences, 2, Betzdorfer Strasse, Köln 50679, Germany
[e] Drohobych Ivan Franko State Pedagogical University, 24, I. Franko Street, Drohobych 82100, Ukraine
[f] Lviv Polytechnic National University, 12, Bandera Street, Lviv 79013, Ukraine

ARTICLE INFO

Article history:
Received 22 September 2014
Received in revised form
11 November 2014
Accepted 17 November 2014
Available online 9 December 2014

Keywords:
Ceramics
Electrical resistance
Stretched exponential relaxation

ABSTRACT

Thermally-induced electronic relaxation in structurally-modified $Cu_{0.1}Ni_{0.8}Co_{0.2}Mn_{1.9}O_4$ spinel ceramics is shown to be adequately described by stretched exponential function on time. This kinetics is defined by microsctructure perfectness of the relaxing media, showing obvious onset to stretched exponential behaviour with non-exponentionality index attaining close to 0.43 values for high-monolith ceramics and smaller ones in fine-grained ceramics. Percolation threshold in relaxation-degradation kinetics is detected for ceramics with 10% of NiO extractions, showing the smallest but most prolonged single-path degradation effect. This finding is treated in terms of Phillips' axiomatic diffusion-to-trap model, where only one of two relaxation channels (caused by operative short-range forces) occurs to be effective, while additional non-operative channels contribute to electronic relaxation in fine-grained ceramics.

1. Introduction

Structural-relaxation effects in disordered solids are known to obey character stretched exponential kinetics in the form of $\sim\exp[-(t/\tau)^{\beta}]$ with *dimensionless stretching exponent* or *non-exponentionality index* $0<\beta<1$. Such stretched exponential relaxation (SER) is under tight attention of materials scientists for a long time, since 1854, the time when Rudolf Hermann Arndt Kohlrausch first observed this law in discharging of Leiden jar [1,2]. Further, in 1863, Friedrich Wilhelm Georg Kohlrausch (the son of Rudolf Kohlrausch) shown that mechanical relaxation is also governed by this kinetics [3]. The SER was rediscovered nearly a century ago, in 1970, by Williams and Watts [4], who used this functional dependence to describe the relaxation kinetics in polymers. So sometimes this type of kinetics is named as Williams–Watts (WW) or Kohlrausch–Williams–Watts (KWW) function. In 1984, Chamberlin et al. [5] were the first who introduced the term "SER" for the Kohlrausch law, which has been remaining valid for now.

During last decades there were numerous attempts to explain possible microscopic origin of SER in different disordered media. One of the first detailed analyses of such microscopic models was given by Klafter et al. in 1986 [6]. In general, these models can be divided on three groups including defect-transfer, hierarchically constrained dynamics and defect-diffusion models.

Defect-transfer model originates from known work of Forster on excitation transfer from donor to static defects [7]. The SER decay in this model was explained as a result of parallel relaxations and hierarchy of distances or, equivalently, the hierarchy of transition rates, leading finally to the weight factor for defect positions and transition rates. This model allowed also the transfer to fractal self-similar structures by introducing fractal dimension instead of a Cartesian one [8].

In 1984, Palmer et al. [9] put forward the model of hierarchically constrained dynamics to explain serial arrangement of elementary relaxation events. The relaxation was imagined to occur in stages with subordinated time scales, the hierarchy of relaxation times being introduced due to constraint imposed by faster degree of freedom before slower can relax (this led in final to the weight factor for relaxation times).

Defect-diffusion model was introduced as an extension on the concept that migrating defects may trigger the relaxation of frozen dipoles in amorphous solids as it was first stated by Glarum in 1960 [10]. By introducing the mean number of distinct sites $S(t)$

* Corresponding author at: Institute of Materials, Scientific Research Company "Carat", 202, Stryjska Street, Lviv 79031, Ukraine.
E-mail address: shpotyuk@novas.lviv.ua (O. Shpotyuk).

http://dx.doi.org/10.1016/j.physb.2014.11.023
0921-4526/

visited by random walker on a lattice, it was shown that this parameter for regular lattices is proportional to $t^{1/2}$ in $D=1$ dimension, to t/lnt in $D=2$ dimensions and to t in $D=3$ dimensions [6]. So in the case of $D=2$, the relaxation occurs to be stretched exponential with non-exponentionality index $\beta=1/2$. Further, Shlesinger and Montroll generalized this approach in 1984 [11], showing that full range of non-exponentially indexes $0<\beta<1$ in the resulting decay function appears owing to the hierarchy of waiting times for defects hopping in a random environment. Thus, in fact, the defect-diffusion model contains parallel decay channels each of them is inherently sequential. This model also allows transition to fractal self-similar structures owing to corresponding replacing of D by spectral or fractal dimension d.

Topological development on microscopic origin of SER was performed at the basis of further extension of above defect-diffusion model as it was done by Lifshitz within his diffusion-to-trap model [12]. This model describes the density of states of electron inserted in a large box of constant potential containing randomly distributed impurities interacting with electron through short-range repulsive potential [13]. Mathematically, such problem is equivalent to the Brownian motion of a particle in the same box with traps or sinks of fixed radius. It is of high importance that both tasks can be solved exactly via typical stretched exponential function having non-exponentionality index $\beta=d/(d+2)$ as inherent topologically-dependent parameter defined by the dimensionality d of configuration space where the relaxation occurs [14,15]. By separating *intrinsic* effects from *extrinsic* ones (produced, in part, by different types of surface contacts and structural inhomogeneities such as aggregated clusters, microscopic and submicroscopic crystallites, etc.), Phillips concluded that the former are dominated by two "magic" numbers, $\beta_{SR}=3/5=0.60$ for relaxation via short-range pathways and $\beta_K=3/7=0.43$ for relaxation via long-range Coulomb forces only [13,16–18].

In the further course, this explanation of the Kohlrausch law was something confused in part that only *short-range* arrangement pathways were shown to be effective in structural relaxation [6,19]. So the first number of $\beta_{SR}=0.60$ simply derived from topological expression $\beta=d/(d+2)$ by assuming that all relaxation paths were equivalently effective in $d=3$ space was ascribed exceptionally to short-range relaxation channel, while the second $\beta_K=0.43$ was given in terms of fractal interpretation for systems having both short- and long-range relaxation inputs, but only a half of which (produced by short-range forces) was efficient in the target relaxing process [19]. The latter approach seems to be more comprehensive with respect to eventual origin of relaxation effects in disordered media. It also remains some possibilities to explain deviations from above "magic" β values owing to external influences and microscopic inhomogeneities in glassy systems in the form of random walks on fractals [20]. Nevertheless the bifurcation of non-exponentionality fractional index β through only one type of forces which can be effective in relaxation, either long- ($\beta=0.43$) or short-range ($\beta=0.6$) ones, are often explored further to explain kinetics behaviour of structural and stress relaxation in oxide glasses [21,22].

The assertion on topological origin of stretched exponential relaxation allows to accept that non-exponentionality index β cannot be presented only as simple fitting parameter in the relaxation kinetics obeying the Kohlrausch low, but rather as meaningful physical value defining topological specifics of relaxation with respect to microscopic channels of relaxation-acting forces involved [23]. It is of high importance that structural-microscopic homogeneity of relaxing media is a necessary condition to observe the bifurcation of stretching exponent β between two "magic" values (0.60 and 0.43). With respect to Phillips's condition for configuration space in disordered systems where relaxation occurs [17], it means separation between extrinsic and intrinsic structural effects, since only the latter are subjected in a strong sense to relaxation through above magic stretching exponents. Moreover, sometimes this bifurcation can be detectable experimentally even in the same homogeneous substance such as fusion-drawn oxide glass affected by stress ($\beta=0.60$) or structural ($\beta=0.43$) relaxation [21]. Nevertheless, the effect of intrinsic and external inhomogneities on SER behaviour is not studied comprehensively up to now. Nothing is known on structural imperfections which can deviate the final relaxation kinetics tending it towards high non-exponentionality (small β values such as 0.1–0.2) or, otherwise, towards single-exponential kinetics ($\beta=1$).

Typically, these microscopically homogeneous disordered media obeying 0.60–0.43 bifurcation in non-exponentionality index β are atomic-continuous electronic and molecular systems like network glasses, where only few kinds of structural imperfections such as coordination defects (or local deviations from full saturation of covalent bonding in the form of oppositely-charged atoms) are possible. The fine-grained ceramics form principally other group of disordered materials, which possess different types of atomic filling under the same chemical composition. Being composed from crystalline grains, more or less developed intergranual boundaries between them and structurally intrinsic pores [24], these solid media stabilized from high-temperature sintering evidently demonstrate wide range of atomic packing from loose to dense one. Such type of ceramics can be well exemplified, in part, by spinel oxymanganites $(Cu,Ni,Co,Mn)_3O_4$ [25–27], which show unique monolithization tendency in dependence on the amount of thermal energy transferred to this system during high-temperature sintering [28]. With this in mind, we shall try to clarify in this work the role of microstructure-chemical perfectness in the electronic relaxation kinetics in these ceramics.

2. Experimental

Bulk samples of oxymanganite spinel-type ceramics of nominal $Cu_{0.1}Ni_{0.8}Co_{0.2}Mn_{1.9}O_4$ composition possessing principally different microstructural perfectness owing to modified step-wise sintering route as it was described in more details elsewhere [28] were examined. Five batches of these ceramics were prepared by varying sintering temperature (from 1040 °C to 1300 °C) and duration (from 60 to 480 min) at nearly the same cooling rate (~8 °C/min). This technological route allows modification of thermal energy transferred during sintering, which results in a wide diversity of ceramics perfectness. The latter was evaluated by amounts of extracted NiO phase (additional to main oxymanganite phase), which was subjected (under the above sintering conditions) to changes from 1% to 12% [28].

Microstructure of the ceramics along with amount of extracted additional NiO phase were controlled by X-ray diffraction patterns recorded at room temperature using HZG-4a powder diffractometer (CuK_α and FeK_α radiation) [27]. Morphological structure of the ceramics chips were probed using electron microscope JSM-6700F (Japan), cross-sections morphology being tested near surface (0–70 μm depth) and deeply in the ceramics bulk.

The prepared ceramics were subjected to degradation tests under prolonged storage (aging) at the elevated temperature of 170 °C lasting defined time intervals (within 10 time domains from 24 to 500 h). Thus, only 10 experimental points were detected for each sample to determine the character of final relaxation kinetics. The results of aging tests were controlled by relative resistance drift (RRD) defined as changes in electrical resistance $\Delta R/R_0$ measured in the normal conditions (near 25 °C and 35% of relative humidity) using a digital multimeter. The confidence interval in the RRD measuring error-bar restricted by equipment inaccuracy was no worse than $\pm 0.2\%$. Additional deviations in some

experimental points were possible due to faults in exact reproduction of degradation cycles in multiple sample-to-sample measurements (cooling regime from the temperature of aging down to the temperature of electrical measurement, influence of environmental atmosphere and humidity, etc.). Statistical analysis testified that above factors introduced additional error of about $\pm 0.2\%$ in the measured $\Delta R/R_0$ values. Therefore, the maximal overall uncertainties in the electrical measurements did not exceed approximately $\pm(0.4-0.5)\%$.

With a purpose of adequate mathematical description of the observed thermally-induced degradation kinetics, the RRD determined by $\Delta R/R_0$ values were simulated by SER function:

$$RRD = a(1 - \exp[-(t/t)^{\beta}]) \quad (1)$$

where a stands for amplitude of degradation effect, τ is effective time constant and β is non-exponentionality fractional index.

The numerical values of different fitting parameters (a, τ and β) in this SER function (1) were calculated in such a way to minimize the mean-square deviations *err* (goodness of fitting) of experimentally measured $\Delta R/R_0$ points from modelling curve. As a result, under accepted uncertainties in $\Delta R/R_0$ measurements, the final accuracy in the value of non-exponentionality index β was ± 0.05.

3. Result and discussion

Oxymanganospinel $Cu_{0.1}Ni_{0.8}Co_{0.2}Mn_{1.9}O_4$ ceramics are known to be one of the most perspective materials for device application as negative temperature coefficient thermistors, temperature sensors, in-rush current limiters, etc. [25]. That is why the problem of their functional stability and exploitation reliability is of high importance.

As a rule, to eliminate parasitic influence of externally-induced degradation effects in such ceramics, the methods of their chemical modification by metallic additives at the initial stages of technological preparation (sintering) has been widely employed [29,30]. Acting as unsaturated gates for induced defects, such metallic additives located near intergranular regions diminish effects of thermally-activated aging due to more stabilized cationic distribution within separate ceramics grains. As a result, the chemically-modified spinel ceramics show higher stability in comparison with non-modified ones.

Principally novel approach to resolve the reliability problem in spinel-type ceramics was outlined in [31]. In part, the additional rock-salt NiO phase, which was not introduced as ingredients at the initial stages of ceramics processing, but only segregated from $Cu_{0.1}Ni_{0.8}Co_{0.2}Mn_{1.9}O_4$ ceramics during high-temperature sintering serves as an effective barrier to inhibit further degradation. The amount of extracted NiO phase occurs a decisive influence on electronic degradation tendencies in the RRD of these ceramics [31], caused by thermal storage at the elevated temperatures such as 170 °C. Thus, chemical inhomogeneities due to extracted NiO phase allow stabilization effect on electrical resistance, provided this trend is significantly coupled with optimized inner morphology of the ceramics.

It is important to note that different types of these spinel ceramics including $Cu_{0.1}Ni_{0.8}Co_{0.2}Mn_{1.9}O_4$ always demonstrate the SER degradation behaviour obeying kinetics under natural aging or other external stimuli in strong respect to Eq. (1), which cannot be substituted by simple single-exponential or bimolecular relaxation kinetics [32].

The morphological specificity of the studied $Cu_{0.1}Ni_{0.8}Co_{0.2}Mn_{1.9}O_4$ ceramics showing significant evolution in their grain-pore microstructure as growing monolithization tendency is well illustrated in Fig. 1.

Typical samples of spinel ceramics from batch no. 1 (Fig. 1a) sintetred at 1040 °C are characterized by ultrafine 1–3 μm grains. Numerous intergranual pores in ceramics body are small enough, their sizes not exceeding 1–2 μm. White spots attributed in respect to the XRD analysis [27,31] to extractions of rock-salt NiO phase (about 1%) appear mainly near intergranual boundaries. Such mictrostructure is known to be caused by minimal level of thermal energy transferred into ceramics body during sintering route arranged above characteristic temperature of monophase $Cu_{0.1}Ni_{0.8}Co_{0.2}Mn_{1.9}O_4$ ceramics (920 °C) [28].

The samples of batch no. 2 ceramics (Fig. 1b) sintered at 1200 °C and more than 1.5 times higher thermally-transferred energy (as compared with batch no. 1 ceramics) have larger separate grains with character ~5–7 μm sizes, some of them reaching ~10 μm. White NiO film (about 8%) appears in these ceramics near intergranual boundaries and inner pore surfaces.

In contrast, the grain-pore microstructure of the ceramics from batch no. 3 (Fig. 1c) sintered at the same maximal temperature (1200 °C), but under nearly 2.7 times higher thermally-transferred energy due to more prolonged stages of thermal treatment (with respect to batch no. 1 ceramics), differs gradually attaining a character highly-monolithized form. The corresponding chip structure of these ceramics is more uniform, being characterized only by some separate ~1–3 μm pores. White NiO film (about 10% with respect to the amount of main $Cu_{0.1}Ni_{0.8}Co_{0.2}Mn_{1.9}O_4$ phase) appears as bright layer of approximately ~10 μm in thickness on the surface of these samples. Reduction in the value of thermally-transferred energy owing to more shortened stages of thermal treatment leads to batch no. 4 ceramics, where some relatively larger pores (near ~3–5 μm) are observed and NiO phase extractions appear as a uniform layer on a whole ceramics surface (about 12% in a total amount). At the same time, with increased sintering temperature (1300 °C) and nearly the same duration of thermal treatment cycles, which is followed by thermally-transferred energy like in case of batch no. 3 ceramics, the prepared ceramics (batch no. 5 in Fig. 1e) are distinguished by complete absence of a characteristic grain structure, these ceramics being intrinsically monolith with only several pores of ~1–3 μm in sizes and surface-extracted NiO film in the amount of 12%.

Thus, the grain-pore microstructure of the studied $Cu_{0.1}Ni_{0.8}Co_{0.2}Mn_{1.9}O_4$ ceramics demonstrate an obviously changed monolithization behaviour in the row of sample batches from fine-grained ceramics (batch nos. 1 and 2) to highly-monolith

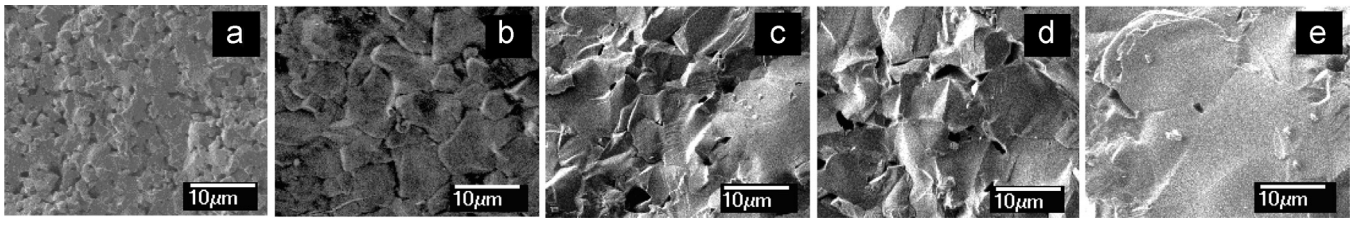

Fig. 1. Morphological structure of $Cu_{0.1}Ni_{0.8}Co_{0.2}Mn_{1.9}O_4$ ceramics of different perfectness defined by amount of extracted NiO phase in the samples from batch no. 1—a (1% NiO), 2—b (8% NiO), 3—c (10% NiO), 4—d (12% NiO) and 5—e (12% NiO).

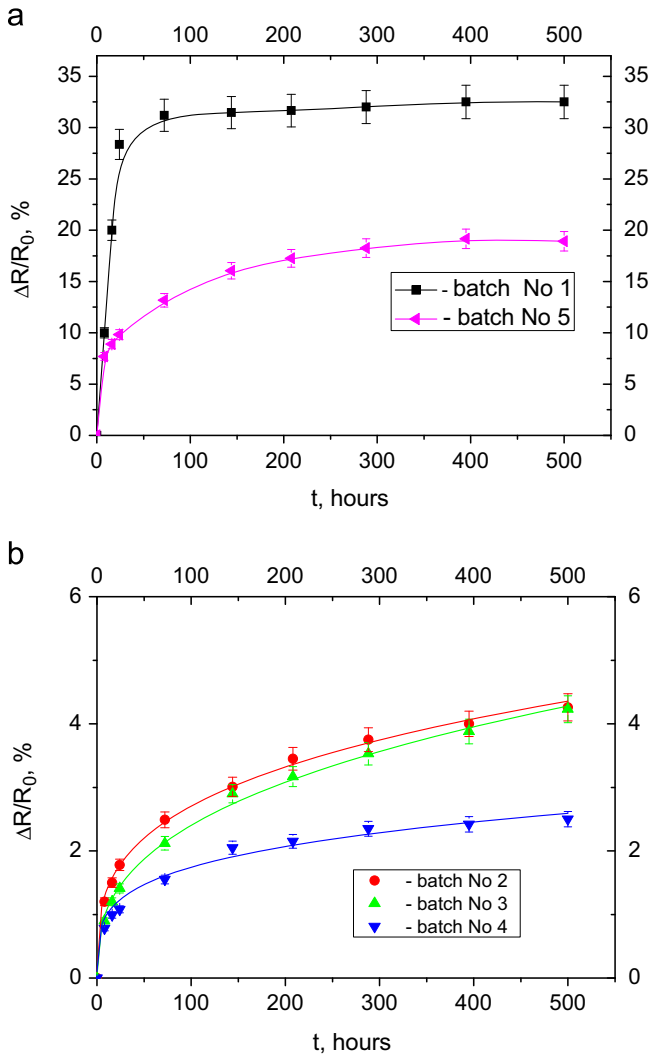

Fig. 2. The RRD ($\Delta R/R_0$) in $Cu_{0.1}Ni_{0.8}Co_{0.2}Mn_{1.9}O_4$ ceramics of different batches. (a—batches nos. 1, 5 and b—batches nos. 2, 3, 4) caused by prolonged storage at 170 °C (the symbols are stand for experimental data and the line represents the SER modelling curve).

ceramics (batch no. 3) and further to most-monolith ceramics (batch no. 5), the batch no. 4 ceramics being considered as partial recovery from monolith towards fine-grained ceramics. In fact, this *microstructure homogenization trend* owing to inner ceramics monolithization is concomitant with *chemical inhomogeneity* caused by amount of extracted NiO phase, which grows essentially from 1% to 12% in the same row of ceramics.

How will these microstructure-chemical homogenization trends be reflected (if any) in the electronic relaxation caused by ceramics exposure under elevated temperature of 170 °C?

Kinetic curves illustrating the RRD defined by $\Delta R/R_0$ values in $Cu_{0.1}Ni_{0.8}Co_{0.2}Mn_{1.9}O_4$ ceramics are shown in Fig. 2. The samples of batch no. 1 having a typical fine-grained inner structure with minimal amount of extracted NiO phase (near 1%) is characterized by the greatest value of RRD achieving more than 30%. With increase in the amount of NiO phase and sizes of ceramics grains (samples of batch no. 2), the saturated RRD value decreased almost to 4.3%. Further decrease in the RRD can be achieved in highly-monolith ceramics. Thus, extremely small value of RRD near 2.5% is character for samples of batch no. 4 (sintered at 1200 °C) having 12% of NiO phase. At the same time, the ceramics of batch no. 5 with the same amount of NiO phase but sintered at higher 1300 °C temperature and, consequently, having more perfect

Table 1
Fitting parameters of SER function (1) describing thermally-induced electronic degradation kinetics in $Cu_{0.1}Ni_{0.8}Co_{0.2}Mn_{1.9}O_4$ ceramics.

Ceramics (NiO content)	$(\Delta R/R_0)_{max}$ (%)	*err*	*a*	β	τ
Batch no. 1 (1% NiO)	32.5	0.123	32.5	0.23	0.5–1.0
Batch no. 2 (8% NiO)	4.3	0.018	6.5	0.39	441.4
Batch no. 3 (10% NiO)	4.2	0.001	9.6	0.43	1766.5
Batch no. 4 (12% NiO)	2.4	0.016	3.1	0.46	189.2
Batch no. 5 (12% NiO)	18.9	0.232	20.8	0.46	65.5

monolith structure, show sharp increase in the RRD up to 18%. The analogous effect is character for ceramics of batch no. 3 having smaller amount of NiO phase (10%) at nearly the same level of monolithization, where the RRD drops to 4.2%. Thus, *chemical inhomogeneities* of the ceramics revealed with extracted NiO phase will cause a blocking effect on the RRD. In other words, we can speculated that an optimal ratio of extracted NiO phase and microstructure monolithization creates an effective channel for electronic relaxation, which effectively suppress degradation effects in the ceramics [28,31].

As to kinetics of these relaxation transformations, all they can be well described by SER function in the form of Eq. (1) with magnitude a defined mainly by amount of extracted NiO phase and non-exponentionality index β dependent strongly on grain-pore morphology of the ceramics (microstructure homogenization). The numerical values of fitting parameters and goodness of fitting (*err* defined as mean-square deviations between experimental points and the modelling curve) for the studied $Cu_{0.1}Ni_{0.8}Co_{0.2}Mn_{1.9}O_4$ ceramics are gathered in Table 1. A number of very important correlations is obvious from careful inspection of these data. Thus, the effective time constant τ in the SER function (1) occurs to be inversely related to the RRD magnitude a, so the quicker relaxation kinetics causes more pronounced degradation in the electrical resistance. Therefore, both processes (increase in the degradation magnitude a and reduction in the τ value) occur to be governed mainly by amount of NiO extractions in the ceramics. Some deviations are proper only to batch no. 4 samples, which do not demonstrate further increase in time constant τ despite a decrease. So phase composition of the ceramics is responsible for rate and magnitude of thermally-induced electronic SER with respect to Eq. (1). At the same time, the fractional exponent β did not reveal any changes, which are in harmony with chemical homogeneity of the ceramics. In fine-grained ceramics of batch no. 1, this parameter was minimal ($\beta=0.23$). Further, it reaches $\beta=0.39$ in the batch no. 2 ceramics with increased grain sizes, approaching the "magic" 0.43 value character for highly-monolith batch no. 3 ceramics. However, it further grows to the same level of $\beta=0.46$ in both most-monolith ceramics from batch no. 5, as well as partially-demonolithized caramics of batch no. 4.

Hence, we conclude that topological appearance of SER with respect to Phillips' axiomatic diffusion-to-trap model [13,16–18] is determined mainly by grain-pore morphology of the studied spinel $Cu_{0.1}Ni_{0.8}Co_{0.2}Mn_{1.9}O_4$ ceramics. The highly-monolith ceramics reveal strong tendency to SER with $\beta=0.43$, which is caused by competitive input of two channels of short- and long-range relaxation-driven forces with an efficient only one of them (the short-range forces). Such forces can be realized only in dense-packed atomic networks proper to ceramics affected by strong space-filling tendencies, when neighbouring separate grains coalescence resulting in disappearing of intergranual pores. In case of extended pore structure and great enough content of fine grains in the ceramics, the structural solidity is significantly destroyed, competitive relaxation channels appearing due to inner multifractal structures. Correspondingly, the non-exponentionality index β decreases in the high-dispersed ceramics of batches nos.

1 and 2, as it was in case of similar processes caused by random walks on fractals [20]. This specificity seems to be responsible for quite small β values observed in the degradation-relaxation processes in other types of fine-grained functional ceramics [30–33].

Therefore, the process of microstructure evolution of the $Cu_{0.1}Ni_{0.8}Co_{0.2}Mn_{1.9}O_4$ spinel ceramics is governed technologically through amount of thermal energy transferred during sintering from high-dispersed porous ceramics revealing small fractional exponents $\beta=0.1$–0.3 to low-dispersed monolith ceramics showing two paths for relaxation with an effective only one of them caused by short-range forces only (which tends the overall kinetics to $\beta=0.43$). Single path for relaxation through effective short-range forces is realized due to NiO extraction accompanied by microstructure monolithization, the percolation threshold being quite close to ceramics with 10% of NiO. These ceramics sample demonstrates the minimal RRD under more prolonged relaxation kinetics with characteristic time constant tending to $\tau=1766.5$ h (Table 1). Structural inhomogeneities are enhanced in both sides with respect to this sample. Below the threshold (in fine-grained ceramics), the competitive relaxation channels are realized due to inner multi-fractal structures, which decrease relaxation times on the costs of RRD magnitude. In over-threshold domain (in most-monolith ceramics), the microstructure perfectness of ceramics is distorted by inhomogeneities in NiO extractions, which act as unsaturated drains for defects also reducing relaxation time constants τ and enhancing magnitude of degradation a. Correspondingly, the *err* in the fitting procedure attains similar deviations, being minimal in case of alone path activated for thermally-induced electronic relaxation in batch no. 3 ceramics (Table 1).

Recently, the successful percolation study in a like manner were performed on many material systems, such as giant metallic domain evolution in VO_2 films on TiO_2 substrate [34], isolated ferromagnetic domain growth in manganite films upon cooling [35], or electrical properties of amorphous $(Co_{45}Fe_{45}Zr_{10})_x(Al_2O_3)_{1-x}$ granular nanocomposites [36]. Direct observation of percolation threshold in the degradation-relaxation kinetics of spinel ceramics in this study was possible due to additional channel, which eliminate structural inhomogeneity of relaxing media. Without this channel of ceramics monolithization, the experiments on electric relaxation where only NiO variations were involved would not be so successful. This situation is like to percolation threshold in the transition temperature of high-temperature superconductors, the effect which was essentially more hidden in its occurrence due to sample inhomogeneities [37–40].

4. Conclusions

The character of thermally-induced electronic degradation in structurally-modified spinel $Cu_{0.1}Ni_{0.8}Co_{0.2}Mn_{1.9}O_4$ ceramics is defined by *microsctructure perfectness* of the relaxing media, showing obvious onset to stretched exponential behaviour with non-exponentionality index attaining close to $3/7=0.43$ values for high-monolith ceramics. This tendency is explained within Phillips' axiomatic diffusion-to-trap model as activation of only one of two operative channels effective for relaxation. The percolation threshold in the observed relaxation-degradation kinetics is detected to be in the ceramics with 10% of NiO extractions, showing the smallest but most prolonged single-path degradation effect.

Acknowledgements

This work was performed in the framework of Agreement on Scientific-Technological Cooperation between Scientific Research Company "Carat" (Lviv, Ukraine) and Fakultät für Informations-, Medien- und Elektrotechnik; Fachhochschule Köln/University of Applied Sciences Cologne (Köln, Deutschland). Sh.O. aknowledges support from the Deutscher Akademischer Austauschdienst (DAAD) for the R&D Project (ref. code A/13/03111) within the "Forschungsaufenthalte" DAAD-programme-2013.

References

[1] R. Kohlrausch, Theorie des Elektrischen Rückstandes in der Leidener Flasche, Pogg. Ann. Phys. Chem. 91 (1854) 179–214.
[2] M. Cardona, R.V. Chamberlin, W. Marx, The history of the stretched exponential function, Ann. Phys. 16 (2007) 842–845.
[3] F. Kohlrausch, Uber die elastische nachwirkung bei der torsion, Pogg. Ann. Phys. Chem. 119 (1863) 337–368.
[4] G. Williams, D.C. Watts, Non-symmetrical dielectric relaxation behaviour arising from a simple empirical decay function, Trans. Farad. Soc. 66 (1790) 80–85.
[5] R.V. Chamberlin, G. Mazurkiewich, R. Orbach, Time decay of the remanent magnetization in spin-glasses, Phys. Rev. Lett. 52 (1984) 867–870.
[6] J. Klafter, M.F. Shlesinger, On the relationship among three theories of relaxation in disordered systems, Proc. Natl. Acad. Sci. U. S. A. 83 (1986) 848–851.
[7] T.Z. Forster, Experimentelle und theoretische Untersuchung des zwischenmolekularen Übergangs von Elektronenanregungsenergie, Naturforsch. Tell. A4 (1949) 321–342.
[8] J. Klafter, A. Blumen, Fractal behavior in trapping and reaction, J. Chem. Phys. 80 (1984) 875–877.
[9] R.G. Palmer, D.L. Stein, E. Abrahams, P.W. Anderson, Models of hierarchically constrained dynamics for glassy relaxation, Phys. Rev. Lett. 53 (1984) 958–961.
[10] S.H. Glarum, Dielectric relaxation of polar liquids, J. Chem. Phys. 33 (1960) 1371–1375.
[11] M.F. Shlesinger, E.W. Montroll, On the Williams–Watts function of dielectric relaxation, Proc Natl. Acad. Sci. U. S. A. 81 (1984) 1280–1283.
[12] I.M. Lifshitz, Energy spectrum strucrure and quantum states of disoredered condensed systems, Usp. Fiz. Nauk 83 (1964) 617–663.
[13] J.C. Phillips, Microscopic theory of the Kohlrausch relaxation constant βK, J. Non-Cryst. Solids 172–174 (1994) 98–103.
[14] H. Scher, M. Lax, Stochastic transport in a disoredered solid. I. Theory, Phys. Rev. B7 (1973) 4491–4502.
[15] P. Grassberger, I.J. Procaccia, The long time properties of diffusion in a mediym with static traps, Chem. Phys. 77 (1982) 6281–6284.
[16] J.P. Phillips, Kohlrausch explained: the solution to a problem that is 150 years old, J. Stat. Phys. 77 (1994) 945–947.
[17] J.C. Phillips, Stretched exponential relaxation in molecular and electronic glasses, Rep. Progr. Phys. 59 (1996) 1133–1207.
[18] J.C. Phillips, Slow dynamics in glasses, Phys. Rev. B73 (2006) 104206-1–104206-6.
[19] J.R. Macdonald, J.C. Phillips, Topological derivation of shape exponent for stretched exponential relaxation, J. Chem. Phys. 122 (2005) 074510-1–074510-8.
[20] P. Jund, R. Jullien, I. Campbell, Random walks on fractals and stretched exponential relaxation, Phys. Rev. E63 (2001) 036131-1–036131-4.
[21] M. Potuzak, R.C. Welch, J.C. Mauro, Topological origin of stretched exponential relaxation in glass, J. Chem. Phys. 135 (2011) 214502-1–214502-7.
[22] R.C. Welch, J.R. Smith, M. Potuzak, X. Guo, B.F. Bowden, T.J. KIczenski, D. C. Allan, E.A. King, A.J. Ellison, J.M. Mauro, Dynamics of glass relaxation at room temperature, Phys. Rev. Lett. 110 (2013) 265901-1–265901-4.
[23] M. Micoulaut, Deep effect of topology on glass relaxation, Physics 6 (2013) 72-1–72-3.
[24] G. Elssner, H. Hover, G. Kiessler, P. Wellner, Ceramics and Ceramic Composites: Materialographic Preparation, Elsevier, 1999 (Amsterdam-Lausanne-New York-Shannon-Singapore-Tokyo).
[25] I.V. Hadzaman, O.I. Shpotyuk, A.P. Kovalskiy, O.Ya Mrooz, Thermal modification of ceramic composites based on manganese cube spinels, Mater. Lett. 29 (1996) 195–198.
[26] O. Shpotyuk, A. Kovalskiy, O. Mrooz, L. Shpotyuk, V. Pechnyo, S. Volkov, Technological modification of spinel-based $Cu_xNi_{1-x-y}Co_{2y}Mn_{2-y}O_4$ ceramics, J. Eur. Ceram. Soc. 21 (2001) 2067–2070.
[27] M. Vakiv, I. Hadzaman, O. Shpotyuk, O. Mrooz, J. Plewa, H. Altenburg, H. Uphoff, O. Bodak, P. Demchenko, On the role of mass-transfer processes in ageing of manganite electroceramics, J. Eur. Ceram. Soc. 24 (2004) 1277–1280.
[28] O. Shpotyuk, V. Balitska, I. Hadzaman, H. Klym, Sintering-modified mixed Ni–Co–Cu oxymanganospinels for NTC electroceramics, J. Alloy. Compd. 509 (2011) 447–450.
[29] R. Metz, M. Brieu, R. Legros, A. Rousset, Intergranular phases in electroceramics, Colloq. de Phys. 51 (1990) 1003–1008.
[30] P. Castelan, A. Bui, A. Loubiere, A. Rousset, R. Legros, Ageing study of NTC thermistors by thermopower measurements, Sens. Actuators A 33 (1992) 119–122.
[31] M.M. Vakiv, O.I. Shpotyuk, V.O. Balitska, B. Butkievich, L.I. Shpotyuk, Ageing behavior of electrical resistance in manganite NTC ceramics, J. Eur. Ceram. Soc. 24 (2004) 1243–1246.

[32] V.O. Balitska, B. Butkiewich, O.I. Shpotyuk, M.M. Vakiv, On the analytical description of ageing kinetics in ceramic manganite-based NTC thermistors, Microelectron. Reliab. 42 (2002) 2003–2007.
[33] H. Klym, V. Balitska, O. Shpotyuk, I. Hadzaman, Degradation transformation in spinel-type functional thick-film ceramic materials, Microelectron. Reliab. 54 (2014) 2843–2848. http://dx.doi.org/10.1016/j.microrel.2014.07.137.
[34] T. Kanki, K. Kawatani, H. Takama, H. Tanaka, Direct observation of giant metallic domain evolution driven by electric bias in VO_2 thin films on TiO_2(001) substrate, Appl. Phys. Lett. 1091 (2012) 243118-1–243118-3.
[35] L. Zhang, C. Israel, A. Biswas, R.L. Greene, A. Lozanne, Direct observation of percolation in a manganite thin film, Science 298 (2002) 805–807.
[36] Yu.E. Kalinin, A.N. Remizov, A.V. Sitnikov, Electrical properties of amorphous $(Co_{45}Fe_{45}Zr_{10})_x(Al_2O_3)_{1-x}$ nanocomposites, Phys. Solid State 46 (2004) 2146–2152.
[37] G. Biankoni, Superconductor-insilator transition on annealed complex networks, Phys. Rev. E85 (2012) 061113-1–061113-5.
[38] G. Biankoni, Superconductor-insilator transition in a network of 2d percolation clusters, Europhys. Lett. A101 (2013) 26003-1–26003-6.
[39] A. Ino, C. Kim, M. Nakamura, T. Yoshida, T. Mizokawa, Z.-X. Shen, A. Fujimori, T. Kakeshita, H. Eisaki, S. Uchida, Electronic structure of $La_{2-x}Sr_xCuO_4$ in the vicinity of the superconductor-insulator transition, Phys. Rev. B62 (2000) 4137-1–4137-5.
[40] D. Lampakis, E. Liarokapis, C. Panagopoulos, Micro-Raman evidence for topological charge order across the superconducting dome of $La_{2-x}Sr_xCuO_4$, Phys. Rev. B73 (2006) 174518-1–174518-12.